Theor Chem Acc (2012) 131:1180
DOI 10.1007/s00214-012-1180-4

REGULAR ARTICLE

Basis set effects on Cu(I) coordination in Cu-ZSM-5: a computational study

Simone Morpurgo · Giuliano Moretti · Mario Bossa

Received: 7 October 2011 / Accepted: 4 January 2012 / Published online: 28 February 2012

Abstract DFT calculations on the coordination of Cu^+ to the framework oxygen atoms of Al-substituted ZSM-5 were performed by using combinations of different basis sets in order to investigate the dependence of the results on the adopted computational level. With low-end basis sets, a large basis set superposition error (BSSE) favors the coordination of Cu^+ to three to four oxygen atoms of the framework, only two of which belong to the AlO_4 tetrahedron corresponding to the investigated T-site. More extended basis sets considerably lower the BSSE and favor the coordination of Cu^+ to only two oxygen atoms of the AlO_4 tetrahedron. Upon interaction with NO, the Cu^+ ion is always coordinated by two oxygen atoms of the AlO_4 tetrahedron, independently of the basis set adopted and of the coordination number before NO adsorption. The shift from three- to twofold coordination caused by the Cu^+–NO interaction requires a deformation energy that lowers the final adsorption energy. Such an effect is relevant with low-end basis sets, whereas it is substantially absent with more extended basis sets, which favor the twofold coordination of Cu^+ even before NO adsorption. As a result, high-end basis sets increase the NO interaction energy with respect to that calculated by low-end basis sets, in agreement with experiments and suggesting a possible re-interpretation of the catalytic properties of the investigated sites. Provided suitable scale factors are employed, the N–O stretching frequencies of adsorbed nitrogen oxide calculated by sufficiently extended basis sets turned out in fair agreement with experimental findings.

S. Morpurgo (✉) · G. Moretti · M. Bossa
Dipartimento di Chimica, Università degli Studi di Roma "La Sapienza", P.le Aldo Moro 5, 00185 Rome, Italy
e-mail: simone.morpurgo@uniroma1.it

Keywords Zeolites · Cu-ZSM-5 · Nitrogen oxide · DFT

1 Introduction

Since its discovery by Iwamoto [1, 2], a huge number of studies was published on Cu-ZSM-5 as a catalyst for NO decomposition, due to its superior activity with respect to other zeolites and supported metal catalysts [3–6]. Nonetheless many points are still under discussion, mainly the nature of active site [7–25] and the reaction mechanism [26–33]. The major problem related to the structural characterization of Cu-ZSM-5, and zeolites in general, is to establish where the Si/Al substitution takes place and how metal cations are coordinated to substituted sites [34, 35]. This point is particularly important since the geometrical features of metal-framework coordination greatly influence the reactivity of the catalyst. Many commonly adopted experimental techniques can give useful information but very seldom they provide unequivocal answers. Theoretical calculations, when coupled to experiments, allow to investigate and to discuss many details that cannot be directly provided by experimental results. The main challenge related to the application of quantum mechanical calculations is to find a compromise between accuracy and computational costs, taking into account that zeolites are complex solids with large unit cells. The most simple and the most complex computational approaches are, respectively, quantum mechanical calculations on small and non-structure-specific cluster models [36–41], or the application of quantum–mechanical methods (mostly based on plane-waves DFT) to the full periodicity of the zeolite lattice [42–50]. Apart from the above two extreme cases, the most widely employed approaches are nowadays molecular orbital calculations which treat only a portion of the

structure (i.e., the active site for a given reaction) taking into account in a variable way the geometrical constraints imposed by the remaining part of the crystal [51, 52]. In this field, the quantum mechanics/molecular mechanics approach (QM/MM) is of particular interest and is commonly adopted either by treating the periodicity of the structure, as in the so-called QM-Pot method [53, 54], or by simply building large clusters that account for the main geometrical features of the material, as in the ONIOM [55–59] method implemented in widely available computer codes. As far as Cu-ZSM-5 is concerned, Sauer and co-workers by means of the above mentioned QM-Pot method investigated the coordination of copper ions within the twelve distinct crystallographic positions of ZSM-5 and calculated the binding energy of Cu^+ [60–62], Cu^{2+} [62] and Cu^+ pairs [63] in different sites and for different coordination numbers. Nachtigall and co-workers, adopting the same computational approach, investigated the adsorption of simple molecules such as CO [44, 64–66], NO [64, 67], NO_2 [64], H_2O [64] and N_2 [64] by Cu-ZSM-5 and Cu-Ferrierite, discussing the interacting ability of Cu^+ ions as a function of their coordination to the zeolite framework. In general, it was shown that, when the Si/Al substitution occurs at the edge of the straight and the sinusoidal channels of ZSM-5, Cu^+ is preferably coordinated by two O atoms of the AlO_4 tetrahedron and points towards the open space at the channels' intersection [60–62]. Such di-coordinated Cu^+ ions have the highest adsorption ability and are expected to be involved in the catalytic activity of Cu-ZSM-5 [68, 69]. However, in many cases, three- or fourfold coordination also occur and compete with the twofold coordination. In particular, it was shown [60, 61, 67] that, when the Si/Al substitution occurs at the T1 position of ZSM-5, the charge-balancing Cu^+ ion can be either twofold coordinated by two oxygen atoms of the AlO_4 tetrahedron or threefold coordinated by two oxygens as in the previous case and by a third oxygen atom located at the opposite side of the ring. The calculated distance between Cu^+ and a fourth oxygen atom at the opposite side of the ring turned out slightly longer than 2.50 Å (the threshold-distance adopted by the authors for coordinative interactions), and for this reason, the latter oxygen was not formally considered as coordinated to Cu^+ [60, 61]. Within the QM-Pot approach, the twofold coordination should be favored by 1.4 kcal mol^{-1} with respect to the threefold one, whereas the shell model potential of the QM-Pot method favors the threefold coordination [60]. Similar calculations were applied to the coordination of Cu^+ to the Al-substituted T7 site of the M7 ring [67]. At difference with the T1 site, only the threefold geometry was predicted for T7. Upon interaction with NO, Cu^+ maintains its coordination to only two oxygen atoms of the AlO_4 tetrahedron which, with the nitrogen atom of NO, form a nearly planar trigonal arrangement around Cu^+. The interaction energy of NO with Cu^+ coordinated at T7, 22.6 kcal mol^{-1} after zero-point energy (ZPE) and basis set superposition error (BSSE) corrections [67] was found to be lower with respect to that calculated for other sites of ZSM-5 where Cu^+ is twofold coordinated even before NO adsorption. The difference, about 7 kcal mol^{-1}, was ascribed to the so-called deformation energy, that is, the energy loss associated to the shift from three- to twofold coordination of Cu^+ with the framework oxygens caused by NO adsorption.

The results obtained by QM/MM methods depend both on the parametrization of the MM part of the code and on the method and basis set adopted in the QM part. In this respect, the above studies were generally performed by DFT methods with similar basis sets, often double-zeta plus polarization for H, Si, Al, Cu and triple-zeta plus polarization for zeolite framework oxygens and adsorbed molecules [60–64, 66, 67]. The aim of the present work is to investigate the coordination of the Cu^+ ion to the T1 and T7 sites of ZSM-5, and its capability to adsorb nitrogen oxide. The above sites are taken as a case study for their possible involvement in the catalytic activity. It is shown how the choice of different basis set combinations affects the computational results, and how literature data could be, in some cases, reconsidered.

2 Computational methods and cluster models

All calculations were performed by the Gaussian-03 code [70]. The B3LYP [71, 72] and PBE1PBE [73–75] functionals were employed, with several combinations of the Ahlrichs' def2-SVP, def2-TZVP and def2-QZVP basis sets [76] for geometry optimization and vibrational analysis. Each basis set, available for all elements from H to Rn with the exclusion of Lanthanides, is consistently designed to give similar errors all across the periodic table. The def2-SVP and def2-TZVP basis sets were developed [76] from the previous default (def- stands for "default") bases of the TURBOMOLE [77] program, which had previously been derived by adding auxiliary functions [78, 79] to the original SVP [80] and TZVP [81] basis sets. The def2-QZVP basis set was developed first for the elements from H to Kr [82] and then for Rb to Rn [76] and, at the same time, it was used to validate [76] the computational results obtained for the less extended def2-SVP and def2-TZVP bases.

The coordination of Cu^+ to the Al-substituted T1 and T7 sites of the so-called M7 ring [60–62, 67] of Cu-ZSM-5 was, respectively, simulated by the $Si_7AlO_{23}H_{14}Cu$ and $Si_9AlO_{29}H_{18}Cu$ clusters, shown in Figs. 1 and 2. The above choice was adopted with the purpose to include in the calculations all first-neighbor T-sites of Al1 and Al7, the

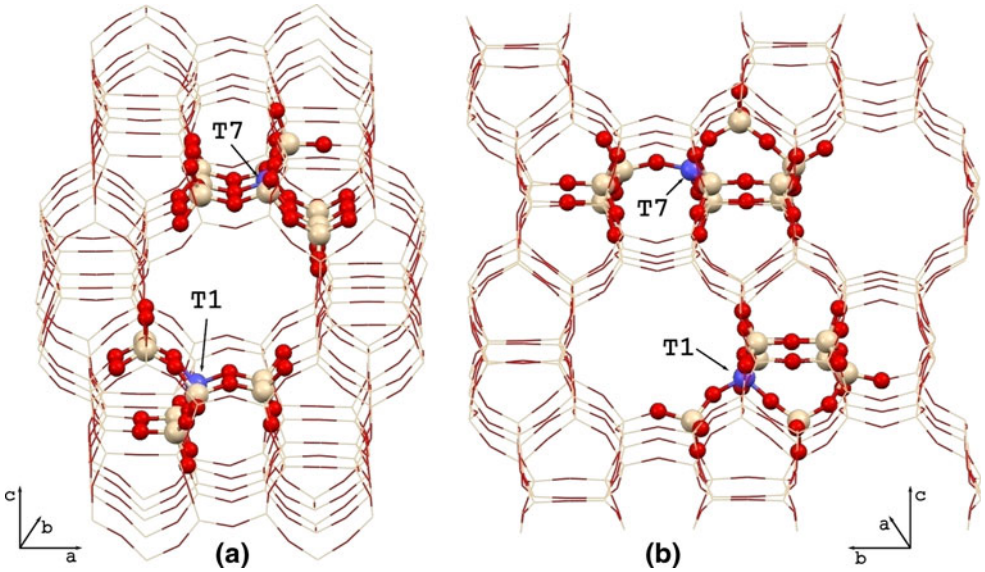

Fig. 1 Location of the investigated clusters within the crystal structure of ZSM-5 [83] viewed **a** along the linear channels and **b** along the sinusoidal channels

M7 ring itself, and at the same time to run geometry optimizations and vibrational analysis at a reasonable cost but with the capability to explore how computational results are affected by the basis set choice. The clusters above are large enough to account for all the interactions of Cu^+ with the zeolite framework as well as for the interactions involved the adsorption of NO. In some cases, the ONIOM [55–59] approach was adopted to check the results obtained by the above cluster calculations.

Although Si7′ in the $Si_9AlO_{29}H_{18}Cu$ cluster (Fig. 2) could be saturated, in principle, by three –OH groups, O7′ and O22′ were actually terminated by $–Si(OH)_3$ residues (Si8′ and Si11′, respectively) to avoid the possible interaction between Cu^+ and –OH groups located in the proximity of Al7. The same problem did not occur for the $Si_7AlO_{23}H_{14}Cu$ cluster, where the saturating –OH groups of Si10 (Fig. 2) have not the right geometrical features to interact with Cu^+ coordinated at the Al1 site. Taking the crystallographic structure of orthorhombic H-ZSM-5 [83] as the starting point, the above clusters were obtained by Si/Al substitution at the chosen T-sites and consequent Cu addition. The total cluster charge was set to zero throughout the calculations, so that a formal Cu^+ ion corresponds to the Al^{3+} ion of the zeolite framework. All saturating H atoms were initially placed 1.0 Å far from the corresponding O, along the bond with the next Si atom not included in the cluster. Geometry optimization was performed in two steps: in the first one, a pre-optimization, all interatomic distances and the Cu^+ coordinates were optimized keeping zeolite bond angles and dihedrals frozen to the corresponding crystallographic values. This was done in order both to adapt the system to the Si/Al substitution and to take into account that DFT calculations slightly overestimate Si–O distances with respect to experimental values [53]. In the second step, the specific ZSM-5 geometry constraints were maintained by freezing all saturating –OH groups in the previously obtained positions. Apart from this, all the remaining geometrical parameters were optimized. The so obtained structures were vibrationally characterized, checking for the absence of imaginary frequencies in the minima. The BSSE was calculated according to the Boys-Bernardi [84] counterpoise method implemented in Gaussian-03. The graphical output of the calculations was obtained by the molecular visualization programs Mercury [85].

3 Results

3.1 Basis set effects on Cu^+ coordination

As shown in Fig. 1, the so-called M7 [60–62, 67] rings of ZSM-5 [83] are located on the walls of the linear channels (which run along the *b* crystal axis) and are, at the same time, at the intersection between linear and sinusoidal channels (the latter ones running along the *a* crystal axis). M7 rings can be considered as the fusion of two five-membered rings of the zeolite framework, respectively, involving the 1-2-8-7-4 and 1-5-11-7-4 T-sites with the 1-4-7 T-sites in common (Fig. 2). Alternatively, they can be viewed as the single 1-2-8-7-11-5 six-membered ring, with the T1 and T7 sites bridged by T4. The ring plane is defined by the 2-8-11-5 T-sites, which are nearly coplanar. Because of the symmetry operations of the *Pnma* space group, the M7 rings are found in pairs along the linear channels. The rings of a given pair are each the specular image of the other one through a mirror plane containing O23 and perpendicular to the channel direction (*b* axis).

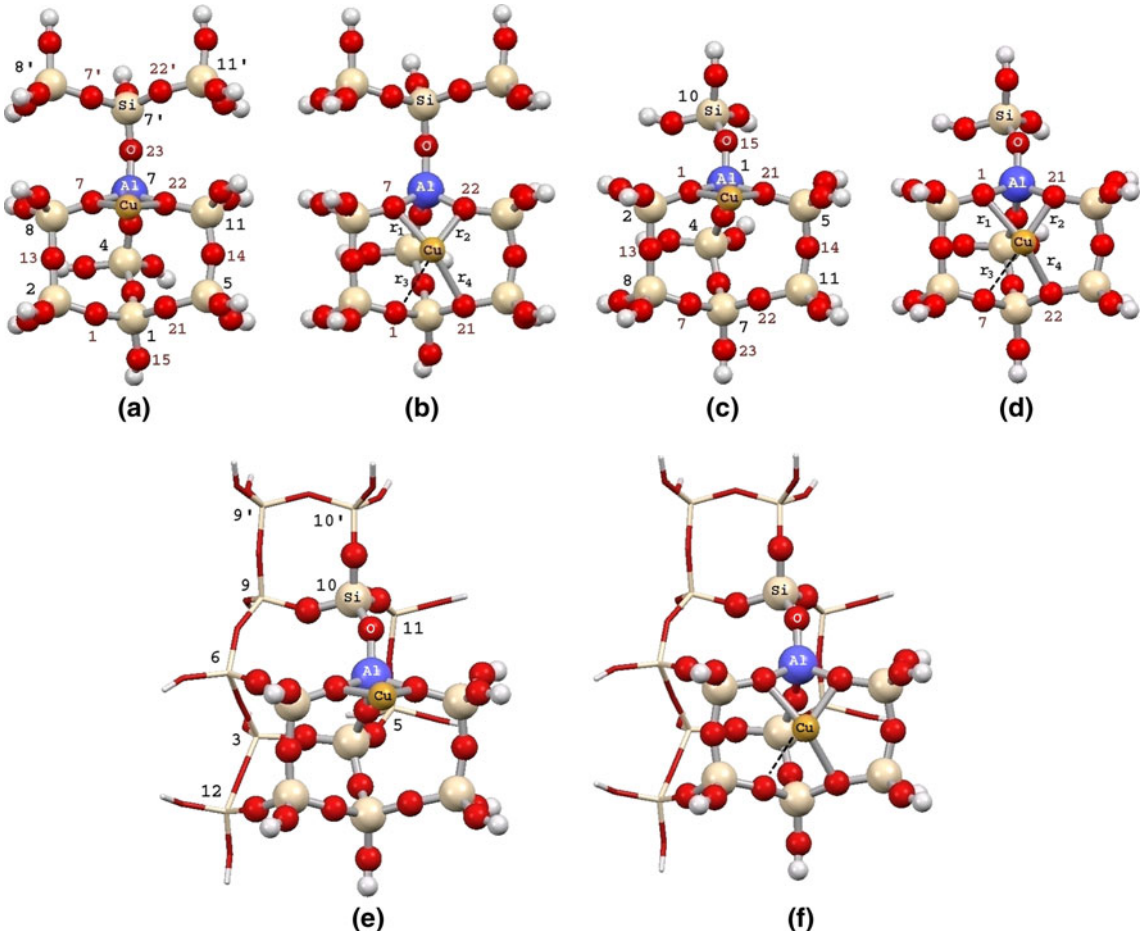

Fig. 2 Investigated clusters representing the coordination of Cu^+ at the Al-substituted T7 and T1 sites of ZSM-5: **a** twofold coordinated at T7; **b** threefold coordinated at T7; **c** twofold coordinated at T1; **d** threefold coordinated at T1; **e** twofold coordinated at T1 in the $Si_{15}AlO_{42}H_{20}Cu$ cluster; **f** threefold coordinated at T1 in the $Si_{15}AlO_{42}H_{20}Cu$ cluster (the atoms represented by balls were treated at the high-level in ONIOM calculations, the ones represented by sticks at the low level). The crystallographic numbering of the most relevant Si and O atoms according to [83] is also shown (notice that Si and O atoms are independently numbered). Selected interatomic distances (see Tables 1 and 2) are also indicated

O23 connects the T7 sites of each ring. Copies of each M7 ring pair are additionally found at the opposite sides of the linear channels, so that the T1 and T7 sites are also at opposite positions across the ten-membered rings that form the walls of the channel itself. T1 sites are exactly at the edge between linear and sinusoidal channels (Fig. 1), whereas T7 sites are part of the common wall of both channels and are also easily accessible.

In the present study, the coordination of Cu^+ to the Al-substituted T7 site of ZSM-5 was investigated first, employing a systematic combination of different basis sets. The calculations were then extended to the T1 site, taking only selected basis sets from those adopted for the T7 site. The main computational results obtained for Cu^+ coordination to the above T-sites are reported in Table 1. Starting from the T7 site, it is shown that when the less extended basis set (def2-SVP on all atoms, indicated as B1) is used for geometry optimization, Cu^+ is threefold coordinated to O7, O22 and O21. The Cu^+–O1 distance (r_3 in Table 1 and Fig. 2) turned out slightly longer than 2.50 Å. In the latter case, adopting the same convention of [60] and [67], Cu^+ was not considered as formally coordinated to O1, but an attractive interaction between the two atoms is anyway likely. It should be mentioned that, when the B1 basis set was employed, the threefold coordination already resulted from the pre-optimization step, even when a twofold coordination was assumed as the starting geometry. The B2 and B3 basis sets differ from B1 for the adoption of the def2-TZVP basis for Cu. They differ from each other because in B2, the simple def2-SV basis (def2-SVP but without *p*-polarization functions) was adopted for H atoms, whereas in B3, hydrogens were again described by the def2-SVP basis. As expected, both bases gave very similar results, with Cu^+ in threefold coordination, and virtually identical Cu^+–O distances. The main difference from B1 calculations was that the pre-optimization gave in both

Table 1 Basis set employed for geometry optimization at investigated T-sites (basis), number of framework oxygen atoms to which Cu^+ is coordinated (n), electronic energy (E/a.u.), zero-point energy (ZPE/a.u.), relative energy of the three- and twofold coordinated structures for a given basis set (E_{rel}/kcal mol^{-1}), basis set superposition error (BSSE/kcal mol^{-1}), selected interatomic distances (r_1, r_2, r_3 and r_4/Å, see Fig. 2) for Cu-zeolite clusters optimized in the present work at selected Al-substituted T-sites of ZSM-5

Basis[a]	n	E	ZPE	E_{rel}	BSSE	r_1	r_2	r_3	r_4
T7 site									
B1	3	−6679.999390	0.084168		13.95	2.19	2.09	2.75	2.48
B2	3	−6680.060617	0.084101		8.28	2.20	2.09	2.77	2.49
B3	3	−6680.238854	0.084130		8.59	2.21	2.09	2.77	2.49
B4	3	−6682.652070	0.083004		11.13	2.19	2.09	2.80	2.54
B5	3	−6682.883754	0.082988	0.00	2.51	2.18	2.08	2.87	2.62
B5	2	−6682.883401	0.083441	0.51	2.06	2.05	2.02	4.36	4.16
B6	3	−6684.083556	0.084469	0.00	1.73	2.19	2.09	2.82	2.56
B6	2	−6684.083020	0.084880	0.59	1.35	2.05	2.02	4.37	4.16
B7	3	−6684.127210	0.084470	0.00	1.59	2.17	2.07	2.85	2.60
B7	2	−6684.127429	0.084886	0.12	1.38	2.05	2.02	4.35	4.14
B7[b]	3	−7200.815037	0.089259	0.00	1.59	2.19	2.08	2.82	2.56
B7[b]	2	−7200.815150	0.089659	0.18	1.37	2.05	2.02	4.35	4.14
B7[c]	3	−6680.138954	0.085239	0.00	1.49	2.19	2.07	2.75	2.49
B7[c]	2	−6680.136190	0.085690	2.02	1.23	2.03	2.00	4.20	3.99
T1 site									
B4	3	−5649.510767	0.066596	0.00	11.56	2.40	2.15	2.71	2.31
B4	2	−5649.507485	0.067280	2.49	8.59	2.04	2.02	4.61	4.42
B7	3	−5650.739752	0.067748	1.52	1.63	2.38	2.15	2.63	2.37
B7	2	−5650.742786	0.068363	0.00	1.34	2.04	2.02	4.71	4.53
B7[c]	3	−5647.509261	0.068428	0.00	1.52	2.40	2.11	2.70	2.26
B7[c]	2	−5647.508167	0.069029	1.06	1.20	2.03	2.01	4.62	4.44
B7[d]	3	−9370.134798	0.161203	0.000		2.26	2.15	2.61	2.37
B7[d]	2	−9370.135406	0.161814	0.001		2.05	2.03	4.61	4.47
B7[e]	3	−9389.508347	0.156569	0.75		2.25	2.15	2.63	2.37
B7[e]	2	−9389.510174	0.157201	0.00		2.05	2.03	4.64	4.49

[a] Basis set definitions: *B1*: H, O, Al, Si, Cu = def2-SVP; *B2*: H = def2-SV; O, Al, Si = def2-SVP; Cu = def2-TZVP; *B3*: H, O, Al, Si = def2-SVP; Cu = def2-TZVP; *B4*: H, Al, Si, Cu = def2-SVP; O = def2-TZVP; *B5*: H, Al, Si = def2-SVP; Cu, O = def2-TZVP; *B6*: H = def2-TZV; O, Al, Si, Cu = def2-TZVP; *B7*: H = def2-TZV; O, Al, Si = def2-TZVP; Cu = def2-QZVP

[b] B3LYP/B7 calculation on a $Si_{10}AlO_{32}H_{20}Cu$ cluster

[c] PBE1PBE/B7 calculation

[d] ONIOM(B3LYP/B7:HF/3-21G) calculation on a $Si_{15}AlO_{42}H_{20}Cu$ cluster

[e] ONIOM(B3LYP/B7:HF/6-311G) calculation on a $Si_{15}AlO_{42}H_{20}Cu$ cluster

cases a twofold Cu^+ coordination (to O7 and O22) even when it was started from the threefold one. In the final geometry optimization, the relaxing of bond angles and dihedrals with respect to the crystallographic values allowed Cu^+ to move toward O21 and to reach the final threefold coordination. Interestingly, during geometry optimization, an energy plateau corresponding to the twofold coordination was observed about 4–5 kcal mol^{-1} above the final energy, but geometry only converged in the threefold coordination. The B4 basis set is similar to that adopted by other authors [60–62, 67], with the def2-SVP basis for H, Al, Si, Cu and the def2-TZVP basis for O atoms. As observed for the B2 and B3 basis sets, the pre-optimization step produced a twofold Cu^+ coordination which shifted to a threefold one in the final optimization, in agreement with literature data [67]. The B5 combination consists of the def2-SVP basis for H, Al, Si and the def2-TZVP basis on both O and Cu. At difference from the B1–B4 basis sets, the latter combination allowed to locate two minima, one corresponding to the already predicted threefold coordination and one displaying a twofold coordination of Cu^+ to O7 and O22, observed before only in the pre-optimization step. The threefold coordinated structure did not show significant geometrical changes with respect to the previous optimizations and was calculated to be more stable than the twofold one by 0.51 kcal mol^{-1},

including the ZPE correction. As shown in Fig. 2 and Table 1, the twofold coordinated structure displays short Cu^+–O7 and Cu^+–O22 distances ($r_1 = 2.05$ and $r_2 = 2.02$ Å, respectively) and much longer Cu^+–O1 and Cu^+–O21 distances ($r_3 = 4.36$ and $r_4 = 4.16$ Å, respectively). Calculations were repeated employing the B6 and, finally, the B7 basis sets, the former one consisting of the full def2-TZVP basis set on all heavy atoms combined with the def2-TZV basis on hydrogens, the latter one differing from B6 for the adoption of the def2-QZVP basis for Cu. The results were qualitatively similar to those obtained by the B5 basis, with an energy gap between the threefold and the twofold structures of 0.59 and 0.12 kcal mol^{-1} at the B6 and at the B7 level, respectively. The calculations performed with the B7 basis were repeated on the larger $Si_{10}AlO_{32}H_{20}Cu$ cluster, in which the –OH group saturating Si7′ in $Si_9AlO_{29}H_{18}Cu$ (Fig. 2) was replaced by the $–Si(OH)_3$ group corresponding to the T4′ site. This was done in order to check whether the increased mobility of Si7′ could affect both the orientation of the AlO_4 tetrahedron in T7 with respect to the plane of the M7 ring and the relative energy of the two minima. Table 1 shows that, with respect to the $Si_9AlO_{29}H_{18}Cu$ cluster, the energy difference between the three- and the twofold geometry increases only from 0.12 to 0.18 kcal mol^{-1}, indicating that the substitution effect is negligible.

The BSSE was calculated for all optimized structures by splitting the system into two subunits, namely the Al-substituted zeolite anion and the Cu^+ cation. As shown in Table 1, a well-defined trend is associated to the just described basis set improvement. For the simple B1 basis, the BSSE is 13.9 kcal mol^{-1}, which represents about 10% of the total binding energy between Cu^+ and the zeolite framework [60]. The adoption of the def2-TZVP basis set for only copper (B2 and B3 bases) reduced the BSSE to about 8.5 kcal mol^{-1}. When the def2-TZVP basis was employed for only oxygen atoms (B4 basis), the BSSE rose again to 11.1 kcal mol^{-1}. The latter two observations suggest the basis set assigned to Cu as the most important in determining the BSSE of the present structures. As the def2-TZVP basis set was assigned to both Cu and O (B5 basis), the BSSE was reduced to about 2.0–2.5 kcal mol^{-1}. The BSSE was further reduced to about 1.3–1.7 kcal mol^{-1} when the def2-TZVP basis was assigned to all heavy atoms (B6 basis). When the def2-QZVP basis set was additionally assigned to copper (B7 basis), a modest BSSE decrease (0.1 kcal mol^{-1}) resulted for the threefold structure only. Calculations performed by the B5, B6 and B7 basis sets also show that the BSSE is always larger for threefold than for twofold coordinated Cu^+, probably as the result of the larger number of Cu^+–O interactions. As a consequence, when the B5–B7 basis sets are adopted, the three- and the twofold coordinated structures turn out virtually isoenergetic after correction for the BSSE.

Calculations on the coordination of Cu^+ to the Al-substituted T1 site of the M7 ring were performed by using the $Si_7AlO_{23}H_{14}Cu$ cluster (Figs. 1 and 2). The B4 and B7 basis sets were selected among those previously employed for the T7 site, either for the sake of comparison with literature data (B4) [60–62, 67] or, in the case of B7, in order to adopt the highest computational level available in the present study. The results are reported in Table 1. As far as Cu^+ coordination is concerned, the main difference with respect to the results obtained for the T7 site is that, even at the B4 level both the threefold and the twofold coordination could be optimized, the former one being more stable by 2.49 kcal mol^{-1} after ZPE correction. The adoption of the more extended B7 basis did not introduce significant geometrical changes in the optimized structures but inverted the relative stability of the two forms, with the twofold coordinated being more stable by 1.52 kcal mol^{-1}. According to literature data [60], both structures could also be optimized by the QM-Pot approach, with a basis set comparable to the B4 one of the present study, the twofold coordinated structure being more stable than the threefold one by 1.4 kcal mol^{-1}. However, it is also reported [61] that, at the same site and by the same computational approach, Cu^+ can be twofold coordinated only in the triplet state, being the threefold coordination more stable in the singlet ground state. Among the above hypothesis, the results of the present work seem to be favorable to the former one.

The BSSE calculated at the B4 level for the structure with threefold coordinated Cu^+ (11.6 kcal mol^{-1}) is very close to that calculated at the same computational level for the corresponding structure at the T7 site, whereas the BSSE calculated at the same level for the twofold coordinated structure (8.6 kcal mol^{-1}) is appreciably lower. The same trend is also observed at the B7 level but, as expected, with lower BSSE values. It is worth mentioning that, if BSSE corrections are applied, at the T1 site, the twofold coordinated structure becomes the most stable (by about 0.5 kcal mol^{-1}) also at the B4 level.

It may be interesting to compare the computational results obtained in the present study for Cu^+ coordination to Al-substituted T1 and T7 sites. It was shown that the twofold coordination of Cu^+ can be obtained at the T1 site employing a less extended basis set (B4) than the basis set (B5) needed to obtain the same coordination at the T7 site. This can be explained by geometrical considerations. Figures 1 and 2 show that the Al1–O15 bond at the T1 site is much more bent out of the M7 ring plane than the Al7–O23 bond at the T7 site. This implies that the AlO_4 tetrahedra associated to the just considered sites have different orientations with respect to the M7 ring plane. In particular,

the O1–Al1–O21 plane at the T1 site (Fig. 2) is almost perpendicular to the ring plane, favoring the twofold coordination of Cu^+. At the T7 site, instead, the angle between the O7–Al7–O22 plane and the ring plane is less than 90° and, very likely, this favors the threefold coordination of Cu^+. Having recognized that the saturation of Si10 by three frozen –OH groups in the $Si_7AlO_{23}H_{14}Cu$ clusters could restrain the mobility of Si10 itself during geometry optimization and, as a consequence, also the orientation of the AlO_4 tetrahedron in T1 with respect to the M7 ring, selected optimizations based on a larger cluster were performed. In this case, owing to the need to saturate the rings located in the nearby region of T1 in ZSM-5, the simple replacement of three –OH groups by $–Si(OH)_3$ groups was not feasible and thus the larger $Si_{15}AlO_{42}H_{20}Cu$ cluster (Fig. 2) had to be adopted. Owing to the cluster size, B3LYP/B7 calculations were found impractical and the ONIOM approach was therefore employed. The $Si_7AlO_{23}H_7Cu$ portion of the system corresponding, with seven saturating hydrogen atoms, to the previous $Si_7AlO_{23}H_{14}Cu$ cluster was treated at the B3LYP/B7 level and the remaining part of the cluster at the HF/3-21G and HF/6-311G levels. Geometry optimizations were performed with the previously described two-step procedure. As shown in Table 1, when the outer part of the cluster is treated at the HF/6-311G level, the twofold coordination of Cu^+ is favored with respect to the threefold one by 0.75 kcal mol^{-1}, whereas the two forms are isoenergetic when the HF/3-21G computational level is adopted. On the whole, the inclusion of a larger portion of the framework does not invert the relative stability of the two forms at T1 but stabilizes the threefold with respect to the twofold coordination of Cu^+.

For the sake of comparison with other computational studies [45–50, 86–88] where the PBE [73, 74] functional was adopted, additional calculations were performed employing the PBE1PBE [75] functional. Such a modified version of the PBE functional includes a 25% of Hartree–Fock exchange and was chosen in order to get results comparable at the same time to those obtained by the pure PBE and by the hybrid B3LYP functionals. Table 1 shows that the PBE1PBE functional favors the threefold coordinated structure both at the the T1 and at the T7 sites by 1.06 and 2.02 kcal mol^{-1}, respectively. A comparison with the corresponding results of B3LYP calculations suggests that the relative stability of the two forms is shifted by about 2 kcal mol^{-1} towards the threefold coordinated one.

3.2 Basis set effects on NO adsorption

The numerical results of NO adsorption on extra-framework Cu^+ are summarized in Table 2. When NO is adsorbed on extra-framework Cu^+ ions in Cu-ZSM-5, mononitrosyl complexes are formed in which Cu^+ is coordinated to the nitrogen atom of NO and to two framework oxygen atoms of the AlO_4 tetrahedron corresponding to the T1 or T7 site (Fig. 3). Such a general geometrical feature of the Cu^+–NO complex is independent of the basis set adopted and of the geometry of Cu^+ before interacting with NO, that is, it is obtained starting the geometry optimization from the originally two- or threefold coordinated Cu^+ sites. In the latter case, the interaction with NO breaks the coordination between Cu^+ and the framework oxygen atoms which do not belong to the AlO_4 tetrahedra (O1/O21 and O7/O22 for Cu^+ coordinated to the Al1 or Al7 site, respectively). This is in agreement with literature data [67]. In addition, two distinct geometries could be optimized for adsorbed NO at a given Cu^+ site (Fig. 3). In one of them indicated as "in", the NO molecule is slightly bent toward the inner part of the M7 ring, in the second one, indicated as "out", NO is bent right in the opposite direction. The just described geometrical feature was also found to be independent of the basis set employed for geometry optimization. The interatomic distances between Cu^+ and the oxygen atoms of the coordinating AlO_4 tetrahedron are short (2.0–2.05 Å, see r_1 and r_2 in Fig. 2 and Table 2) and nearly independent of the basis set employed. The distances between Cu^+ and O1/O21 or O7/O22 are instead longer (from 3.65 to 4.63 Å, see r_3 and r_4 in Fig. 2 and Table 2) and tend to increase at increasing basis set extension (i.e., from B1 to B7). For a given basis set, the r_1 distance is always longer than r_2 and r_3 is always longer than r_4. Finally, for a given basis set, Cu^+ coordination to Al1 results in longer r_3 and r_4 distances than Cu^+ coordination to Al7. The latter feature can be ascribed to the already discussed orientation of the respective AlO_4 tetrahedra with respect to plane of the M7 ring. The adsorption energies of NO on coordinated Cu^+ showed a peculiar dependence on the basis set applied. As a foreword, the basis set dependence of the BSSE should be analyzed. When the B1 basis set is applied, the BSSE is large, about 5.7–6.0 kcal mol^{-1}, which is more than 20% of the final interaction energy. With the B2 and B3 basis sets (where the def2-TZVP basis set was adopted for Cu^+ and adsorbed NO), the BSSE was found to decrease to about 2.1 kcal mol^{-1}. Changing the basis from B3 to B3′ (where adsorbed NO was again described by the def2-SVP basis), the BSSE rose to 3.8 kcal mol^{-1}. By means of the B4 basis, where the TZVP basis was only assigned to N and all O atoms, a BSSE of 4.5 kcal mol^{-1} turned out. The latter findings show that, to achieve a small BSSE, a TZVP-level basis is required for both Cu and adsorbed NO, but the role played by the basis set assigned to Cu is somewhat more important, as it was already shown for the coordination of Cu^+ to the zeolite framework. The adoption of the def2-TZVP basis for N, O and Cu (B5) resulted

Table 2 Basis set employed for geometry optimization at the investigated T-sites (basis), orientation of adsorbed NO molecule (*or*. see text and Fig. 3), electronic energy (*E*/a.u.), zero-point energy (*ZPE*/a.u.), basis set superposition error (BSSE/kcal mol^{-1}), deformation energy (E_{def}/kcal mol^{-1}, see text), NO adsorption energy (E_{ads}/kcal mol^{-1}), BSSE-corrected NO adsorption energy ($E_{ads,BSSE}$/kcal mol^{-1}), selected interatomic distances (r_1, r_2, r_3 and r_4/Å, see Fig. 2), Cu^+−N distance (r_{Cu-N}/Å), N–O distance (r_{N-O}/Å), N–O stretching frequency (ν_{N-O}/cm^{-1}) calculated for NO adsorbed on the Cu-zeolite clusters optimized in the present work at selected Al-substituted T-sites of ZSM-5

Basis[a]	*Or.*	*E*	*ZPE*	BSSE	E_{def}	E_{ads}	$E_{ads,BSSE}$	r_1	r_2	r_3	r_4	r_{Cu-N}	r_{N-O}	ν_{N-O}
T7 site														
B1	In	−6809.833590	0.091455	6.06	4.77	−26.60	−20.54	2.03	2.00	3.87	3.65	1.815	1.158	1826[d]
B1	Out	−6809.833158	0.091434	5.74	4.96	−26.34	−20.61	2.03	2.00	3.94	3.73	1.815	1.159	1823[d]
B2	In	−6810.049127	0.091145	2.13	3.14	−24.31	−22.17	2.04	2.00	4.09	3.87	1.799	1.156	1818[e]
B2	Out	−6810.048952	0.091132	2.03	3.15	−24.21	−22.18	2.03	2.00	4.14	3.92	1.799	1.157	1813[e]
B3	In	−6810.227231	0.091176	2.17	3.25	−24.22	−22.05	2.04	2.00	4.09	3.87	1.799	1.156	1818[e]
B3	Out	−6810.227050	0.091161	2.07	3.26	−24.12	−22.05	2.04	2.00	4.13	3.91	1.800	1.157	1814[e]
B3′	In	−6810.072363	0.091334	3.81	3.23	−26.22	−22.41	2.04	2.00	4.06	3.84	1.805	1.159	1814[d]
B3′	Out	−6810.072182	0.091326	3.79	3.25	−26.11	−22.32	2.03	2.00	4.14	3.92	1.804	1.160	1810[d]
B4	In	−6812.642118	0.089966	4.53	3.04	−25.33	−20.79	2.04	2.01	4.18	3.96	1.809	1.154	1832[e]
B4	Out	−6812.642081	0.089976	4.52	3.07	−25.30	−20.78	2.04	2.01	4.21	4.00	1.808	1.155	1829[e]
B5	In	−6812.873696	0.089969	1.02	0.58	−25.25	−24.22	2.05	2.01	4.28	4.06	1.805	1.155	1822[e]
B5	Out	−6812.873617	0.089965	1.01	0.58	−25.20	−24.19	2.04	2.01	4.29	4.08	1.805	1.155	1818[e]
B6	In	−6814.073224	0.091394	0.86	0.70	−25.11	−24.25	2.05	2.01	4.27	4.05	1.805	1.155	1820[e]
B6	Out	−6814.073171	0.091392	0.86	0.69	−25.08	−24.22	2.04	2.01	4.29	4.08	1.805	1.156	1816[e]
B7	In	−6814.118361	0.091420	0.65	0.22	−26.03	−25.38	2.04	2.00	4.29	4.07	1.803	1.156	1814[e]
B7	Out	−6814.118366	0.091425	0.64	0.22	−26.03	−25.39	2.04	2.00	4.30	4.08	1.803	1.156	1812[e]
B7[b]	In	−6809.987758	0.092434	0.60	2.10	−24.89	−24.28	2.02	1.99	4.10	3.88	1.788	1.149	1824[f]
B7[b]	Out	−6809.987671	0.092429	0.60	2.12	−24.84	−24.23	2.02	1.99	4.13	3.92	1.787	1.150	1822[f]
T1 site														
B4	in	−5779.501692	0.073698	4.69	2.47	−25.79	−21.10	2.04	2.02	4.59	4.40	1.806	1.155	1830[e]
B4	out	−5779.501625	0.073699	4.67	2.48	−25.75	−21.08	2.04	2.02	4.61	4.43	1.806	1.155	1829[e]
B7	in	−5780.733172	0.074871	0.60	0.39	−25.82	−25.22	2.04	2.01	4.63	4.44	1.803	1.156	1812[e]
B7	out	−5780.733163	0.074880	0.58	0.39	−25.81	−25.23	2.04	2.01	4.64	4.45	1.804	1.157	1811[e]
B7[b]	in	−5777.359106	0.075723	0.56	1.11	−25.48	−24.92	2.02	1.99	4.51	4.32	1.787	1.150	1822[f]
B7[b]	out	−5777.359057	0.075724	0.55	1.11	−25.45	−24.90	2.02	1.99	4.53	4.34	1.787	1.150	1820[f]
B7[c]	in	−9500.125125	0.168320		0.05	−25.40		2.04	2.02	4.53	4.37	1.808	1.155	1819[e]
B7[c]	out	−9500.125082	0.168326		0.05	−25.37		2.04	2.02	4.54	4.38	1.808	1.155	1819[e]

[a] Basis set definitions: *B1*: H, N, O, Al, Si, Cu, = def2-SVP; *B2*: H = def2-SV; O, Al, Si = def2-SVP; Cu, NO_{ads} = def2-TZVP; *B3*: H, O, Al, Si = def2-SVP; Cu, NO_{ads} = def2-TZVP; *B3′*: H, N, O, Al, Si = def2-SVP; Cu = def2-TZVP; *B4*: H, Al, Si, Cu = def2-SVP; N, O = def2-TZVP; *B5*: H, Al, Si = def2-SVP; N, O, Cu = def2-TZVP; *B6*: H = def2-TZV; N, O, Al, Si, Cu = def2-TZVP; *B7*: H = def2-TZV; N, O, Al, Si = def2-TZVP; Cu = def2-QZVP

[b] The PBE1PBE functional was employed

[c] ONIOM(B3LYP/B7:HF/3-21G) calculation on a $Si_{15}AlO_{42}H_{20}Cu$ cluster

[d] The ν(exp)/ν(calc) 1904/2042 = 0.9324 scaling factor was applied

[e] The ν(exp)/ν(calc) 1904/1977 = 0.9631 scaling factor was applied

[f] The ν(exp)/ν(calc) 1904/2031 = 0.9375 scaling factor was applied

in a BSSE of 1.0 kcal mol^{-1}. The assignment of the full def2-TZVP basis to all heavy atoms (B6) and the further addition of the def2-QZVP basis to Cu (B7) resulted in a BSSE decrease to about 0.85 and 0.65 kcal mol^{-1}, respectively. At difference from the BSSE, the adsorption energy uncorrected for the BSSE (from about 24 to 26 kcal mol^{-1}) is characterized by little changes from one basis set to another, with the highest values obtained for B1, B3′ and B7, respectively. Such a behavior should not be surprising because it arises from a compromise between two opposite factors, namely the BSSE and the so-called deformation energy. The latter parameter is assumed as the difference between the electronic energy of each cluster, obtained from a single-point calculation after NO removal,

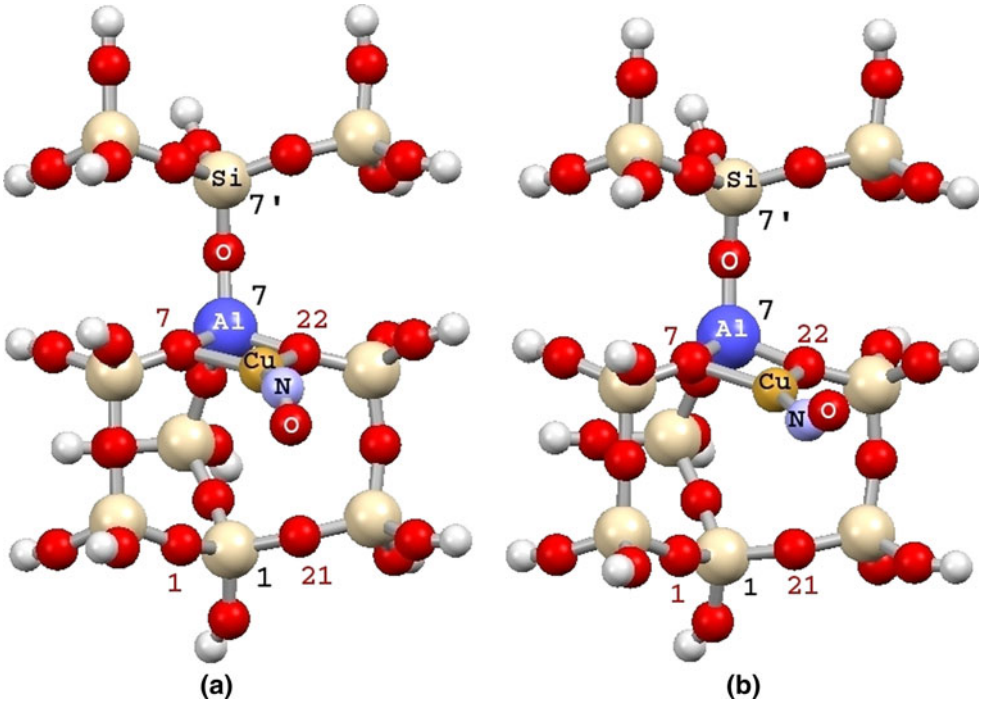

Fig. 3 Investigated clusters representing the adsorption of NO by Cu^+ coordinated at the T7 site of Al-substituted ZSM-5. The "in" (**a**) and "out" (**b**) orientations of the adsorbed NO molecule with respect to the M7 ring (see Text and Table 2) are indicated. The geometrical features of NO adsorption on Cu^+ coordinated at the T1 site are equivalent

and that of the most stable conformation of the corresponding cluster optimized before NO adsorption. The computed values, reported in Table 2, show a trend which resembles that of the BSSE. This implies that (1) when low-end basis sets (from B1 to B4) were employed, before NO adsorption only the threefold coordinated structure could be optimized for Cu^+ at the T7 site. After NO adsorption, the deformation energy associated to the shift of Cu^+ from three- to twofold coordination to the framework oxygens was compensated by the BSSE associated to the Cu^+–NO interaction. (2) When high-end basis sets (B5-B7) were adopted, the two- and the threefold coordination of Cu^+ to the zeolite framework turned out nearly isoenergetic before NO adsorption at the T7 site, and the twofold coordination was shown to be the preferred one at the T1 site. As a consequence, a low deformation energy was involved in the interaction with NO. At the same time, extended basis sets allowed the computation of the interaction energy with a small BSSE, giving similar values as those calculated by low-end basis sets.

The true basis set dependence of the Cu^+–NO interaction energy could finally be appreciated once corrections for the BSSE were applied. When the less extended basis sets were employed, the large BSSE calculated (up to 6 kcal mol^{-1}) decreased the corresponding adsorption energies even to 20–21 kcal mol^{-1}. The small BSSE values calculated instead by means of larger basis sets (B6 and B7) decreased the corresponding interaction energies by no more than 0.6–0.8 kcal mol^{-1}, resulting in final adsorption energies close to 25.5 kcal mol^{-1}, in good agreement with the experimental value of about 24 kcal mol^{-1} [89]. Negligible differences (0.3–0.4 kcal mol^{-1}, Table 2) in the adsorption energy of NO were observed when PBE1PBE calculations were performed at the T1 and T7 sites, and when larger clusters (ONIOM B3LYP/B7:HF/3-21G calculations) were employed to simulate NO adsorption at the T1 site.

3.3 NO stretching frequency

The stretching frequency of the N–O bond after adsorption by the zeolite-coordinated Cu^+ ion can be computed and compared with easily available experimental data. The present computational results are shown in Table 2. As a starting point, the calculated N–O stretching frequencies of gas-phase nitrogen oxide turned out to be 2042 and 1977 cm^{-1} at the B3LYP/def2-SVP and B3LYP/def2-TZVP computational level, respectively. A comparison with the experimental frequency of 1904 cm^{-1} [90], allowed to calculate the corresponding ν(exp)/ν(calc) scale factors equal to 0.9324 and 0.9631, respectively. As reported in Table 2, the application of such scale factors to the calculated frequencies of adsorbed NO resulted in scaled frequencies in good agreement with the experimental value of 1,810–1,812 cm^{-1} [13, 91], whenever the def2-TZVP basis is assigned to Cu (i.e., with the exceptions of the B1 and B4 bases). For the B7 basis, in particular, the scaled frequencies are virtually coincident with the experimental ones, at both the T1 and T7 sites, providing in this way a valuable tool for the interpretation of

many spectroscopic data available in the literature. As also shown in Table 2, PBE1PBE/B7 calculations resulted in slightly larger values of the nitrogen oxide stretching frequency, both in the gas-phase (2,031 cm^{-1}) and after adsorption (about 1,820 cm^{-1}, with application of the corresponding 0.9375 scale factor). A value of about 1,820 cm^{-1} was also calculated when the ONIOM scheme was applied to simulate the adsorption of NO at the T1 site.

4 Discussion and conclusions

The present calculations showed that the computationally predicted coordination of Cu^+ to the framework of Al-substituted T1 and T7 sites of Cu-ZSM-5 depends on the geometrical features of the considered sites and also on the computational level adopted, being particularly sensitive to the basis set employed. The observed trend among different basis sets of increasing complexity could be rationalized by admitting that, when a valence double-zeta basis set (def2-SVP) is employed for geometry optimization, large BSSE effects push Cu^+ towards higher coordination to framework oxygens, in particular towards a threefold geometry where one of the coordinating oxygens is located at the opposite side of the M7 ring with respect to the AlO_4 tetrahedron. In such a way, the Cu^+ ion and the coordinating oxygen atoms of the zeolite framework, being at a short distance, display an increased ability to lower the system energy by sharing the respective basis functions. When a more extended basis set is adopted, at least triple-zeta plus polarization functions (def2-TZVP) for both copper and oxygen, the tendency of Cu^+ to higher coordination decreases as a consequence of a lower BSSE. As a result, for Cu^+ exchanged at the T7 site, a twofold coordinated structure could additionally be optimized with respect to literature data [67], turning out isoenergetic as the already characterized threefold one. In a similar way, for Cu^+ at the T1 site, the corresponding twofold structure, also predicted by means of less extended basis sets [60] gained relative stability with respect to the threefold one, resulting as the most stable minimum.

The coordination of Cu^+ to the zeolite framework was also shown to affect the energetics of NO adsorption. A calculated interaction energy of 22.6 kcal mol^{-1} was previously reported [67] for the Cu^+–NO interaction at the Al-substituted T7 site of Cu-ZSM-5. On this basis, it was suggested that this and similar sites (such as T1) could be less reactive than other sites (T3, T6, T9 and T12) located at the edge between linear and sinusoidal channels, for which an interaction energy up to 29 kcal mol^{-1} was instead calculated [67]. The different behavior of the considered sites was ascribed to the coordination of Cu^+ before NO adsorption (threefold for T7, both two and threefold for T1, and twofold for T3, T6, T9 and T12) and to the deformation energy required by threefold coordinated Cu^+ ions to lose one Cu^+–O coordination bond and to form the Cu^+–NO complex. The present calculations showed instead that, once a triple-zeta plus polarization basis set is employed and by virtue of the just described geometries and energetics of Cu^+ coordination at the T1 and T7 sites, no deformation energy is required for the Cu^+–NO interaction to take place. After BSSE correction, a NO adsorption energy of about 25.5 kcal mol^{-1} was finally calculated at the considered sites. To afford a fully consistent comparison between the nitrogen oxide adsorption capability of Al-substituted T1 and T7 sites with that of other T-sites in which Cu^+ is twofold coordinated (T3, T6, T9 and T12), the computational approach of the present work should obviously be extended to the latter sites. As a final remark, it appears that the PBE1PBE functional tends to favor the stability of threefold coordinated structures with respect to the twofold ones (which could anyway be optimized in the present work) for Cu^+ in ZSM-5. Such a tendency is also reported in the literature [86–88] for the pure PBE functional.

As a conclusion, the present analysis shows that the computational level and the basis set adopted in the calculations may have a crucial importance in the prediction of the structural and catalytic properties of Cu-ZSM-5, not only in terms of the final numerical results of computed observables, but also in terms of a physical description of the phenomena as the sum of different and variable contributions.

References

1. Iwamoto M, Yoko S, Sakai K, Kagawa S (1981) J Chem Soc, Faraday Trans I(77):1629–1638
2. Iwamoto M, Furukawa H, Mine Y, Uemura F, Mikuriya S, Kagawa S (1986) J Chem Soc Chem Commun 1272–1273
3. Iwamoto M, Hamada H (1991) Catal Today 10:57–71
4. Shelef M (1995) Chem Rev 95:209–225
5. Pârvulescu VI, Grange P, Delmon B (1998) Catal Today 46:233–317
6. Garin F (2001) Appl Catal A 222:183–219
7. Li Y, Hall WK (1991) J Catal 129:202–215
8. Valyon J, Hall WK (1993) Catal Lett 19:109–119
9. Moretti G (1994) Catal Lett 28:143–152
10. Campa MC, Indovina V, Minelli G, Moretti G, Pettiti I, Porta P, Riccio A (1994) Catal Lett 23:141–149
11. Spoto G, Bordiga S, Ricchiardi G, Scarano D, Zecchina A, Geobaldo F (1995) J Chem Soc, Faraday Trans 91:3285–3290
12. Lei GD, Adelman BJ, Sárkány J, Sachtler WMH (1995) Appl Catal B 5:245–256
13. Beutel T, Sárkány J, Lei GD, Yan JY, Sachtler WMH (1996) J Phys Chem 100:845–851
14. Lo Jacono M, Fierro G, Dragone R, Feng X, d'Itri J, Hall WK (1997) J Phys Chem B 101:1979–1984
15. Recchia S, Dossi C, Psaro R, Fusi A, Ugo R, Moretti G (2002) J Phys Chem B 106:13326–13332

16. Modén B, Da Costa P, Fonfé B, Lee DK, Iglesia E (2002) J Catal 209:75–86
17. Da Costa P, Modén B, Meitzner GD, Lee DK, Iglesia E (2002) Phys Chem Chem Phys 4:4590–4601
18. Modén B, Da Costa P, Lee DK, Iglesia E (2002) J Phys Chem B 106:9633–9641
19. Groothaert MH, van Bokhoven JA, Battiston AA, Weckhuysen BM, Schoonheydt RA (2003) J Am Chem Soc 125:7629–7640
20. Kuroda Y, Iwamoto M (2004) Topics Catal 28:111–118
21. Moretti G, Ferraris G, Fierro G, Lo Jacono M, Morpurgo S, Faticanti M (2005) J Catal 232:476–487
22. Serikh AI, Amiridis MD (2006) Microporous Mesoporous Mater 94:320–324
23. Itadani A, Tanaka M, Mori T, Nagao M, Kobayashi H, Kuroda Y (2007) J Phys Chem C 111:12011–12023
24. Itadani A, Sugiyama H, Tanaka M, Mori T, Nagao M, Kuroda Y (2007) J Phys Chem C 111:16701–16705
25. Smeets PJ, Sels BF, van Teeffelen RM, Leeman H, Hensen EJM, Schoonheydt RA (2008) J Catal 256:183–191
26. Trout BL, Chakraborty AK, Bell AT (1996) J Phys Chem 100:4173–4179
27. Bell AT (1997) Catal Today 38:151–156
28. Schneider WF, Hass KC, Ramprasad R, Adams JB (1997) J Phys Chem B 101:4353–4357
29. Ramprasad R, Hass KC, Schneider WF, Adams JB (1997) J Phys Chem B 101:6903–6913
30. Tajima M, Hashimoto M, Toyama F, El-Nahas AM, Irao K (1999) Phys Chem Chem Phys 1:3823–3830
31. Sengupta D, Adams JB, Schneider WF, Hass KC (2001) Catal Lett 74:193–199
32. Solans-Monfort X, Branchadell V, Sodupe M (2002) J Phys Chem B 106:1372–1379
33. Solans-Monfort X, Sodupe M, Branchadell V (2003) Chem Phys Lett 368:242–246
34. Bulánek B, Čičmanec P, Knotek P, Nachtigallová D, Nachtigall P (2004) Phys Chem Chem Phys 6:2003–2007
35. Sklenak S, Dědeček J, Li C, Wichterlová B, Gábová V, Sierka M, Sauer J (2009) Phys Chem Chem Phys 11:1237–1247
36. Schneider WF, Hass KC, Ramprasad R, Adams JB (1996) J Phys Chem 100:6032–6046
37. Hass KC, Schneider WF (1996) J Phys Chem 100:9292–9301
38. Ramprasad R, Schneider WF, Hass KC, Adams JB (1997) J Phys Chem B 101:1940–1949
39. Goodman BR, Schneider WF, Hass KC, Adams JB (1998) Catal Lett 56:183–188
40. Rodriguez-Santiago L, Sierka M, Branchadell V, Sodupe M, Sauer J (1998) J Am Chem Soc 120:1545–1551
41. Hass KC, Schneider WF (1999) Phys Chem Chem Phys 1:639–648
42. Filippone F, Buda F, Iarlori S, Moretti G, Porta P (1995) J Phys Chem 99:12883–12891
43. Bludský O, Nachtigallová D, Bulánek R, Nachtigall P (2005) Stud Surf Sci Catal 158:625–632
44. Bludský O, Šilhan M, Nachtigall P, Bucko T, Benco L, Hafner J (2005) J Phys Chem B 109:9631–9638
45. Otero Areán CO, Turnes Palomino G, Llop Carayol MR, Pulido A, Rubeš M, Bludský O, Nachtigall P (2009) Chem Phys Lett 477:139–143
46. Pulido A, Nachtigall P (2009) Phys Chem Chem Phys 11:1447–1458
47. Pulido A, Delgado MR, Bludský O, Rubeš M, Nachtigall P, Areán CO (2009) Energy Environ Sci 2:1187–1195
48. Bulánek R, Voleská I, Ivanova E, Hadjiivanov K, Nachtigall P (2009) J Phys Chem C 113:11066–11076
49. Grajciar C, Areán CO, Pulido A, Nachtigall P (2010) Phys Chem Chem Phys 12:1497–1506
50. Bulánek R, Frolich K, Čičmanec P, Nachtigallová D, Pulido A, Nachtigall P (2011) J Phys Chem C 115:13312–13321
51. Goodman BR, Hass KC, Schneider WF, Adams JB (1999) J Phys Chem B 103:10452–10460
52. Zheng X, Zhang Y, Bell AT (2007) J Phys Chem C 111:13442–13451
53. Sierka M, Sauer J (1997) Faraday Discuss 106:41–62
54. Sauer J, Sierka M (2000) J Comput Chem 21:1470–1493
55. Maseras M, Morokuma K (1995) J Comp Chem 16:1170–1179
56. Svensson M, Humbel S, Morokuma K (1996) J Chem Phys 105:3654–3661
57. Svensson M, Humbel S, Froese RDJ, Matsubara T, Sieber S, Morokuma K (1996) J Phys Chem 100:19357–19363
58. Dapprich S, Komáromi I, Byun KS, Morokuma K, Frisch MJ (1999) J Mol Struct (Theochem) 462:1–21
59. Vreven T, Morokuma K (2000) J Comp Chem 21:1419–1432
60. Nachtigallová D, Nachtigall P, Sierka M, Sauer J (1999) Phys Chem Chem Phys 1:2019–2026
61. Nachtigall P, Nachtigallová D, Sauer J (2000) J Phys Chem B 104:1738–1745
62. Nachtigallová D, Nachtigall P, Sauer J (2001) Phys Chem Chem Phys 3:1552–1559
63. Spuhler P, Holthausen MC, Nachtigallová D, Nachtigall P, Sauer J (2002) Chem Eur J 8:2099–2115
64. Nachtigall P, Davidová M, Šilhan M, Nachtigallová D (2002) Stud Surf Sci Catal 142:101–108
65. Bludský O, Šilhan M, Nachtigallová D, Nachtigall P (2003) J Phys Chem A 107:10381–10388
66. Davidová M, Nachtigallová D, Bulánek R, Nachtigall P (2003) J Phys Chem B 107:2327–2332
67. Davidová M, Nachtigallová D, Nachtigall P, Sauer J (2004) J Phys Chem. B 108:13674–13682
68. Dědeček J, Wichterlová B (1999) Phys Chem Chem Phys 1:629–637
69. Nachtigall P, Davidová M, Nachtigallová D (2001) J Phys Chem B 105:3510–3517
70. Frisch MJ, Trucks GW, Schlegel HB, Scuseria GE, Robb MA, Cheeseman JR, Montgomery JA Jr, Vreven T, Kudin KN, Burant JC, Millam JM, Iyengar SS, Tomasi J, Barone V, Mennucci B, Cossi M, Scalmani G, Rega N, Petersson GA, Nakatsuji H, Hada M, Ehara M, Toyota K, Fukuda R, Hasegawa J, Ishida M, Nakajima T, Honda Y, Kitao O, Nakai H, Klene M, Li X, Knox JE, Hratchian HP, Cross JB, Bakken V, Adamo C, Jaramillo J, Gomperts R, Stratmann RE, Yazyev O, Austin AJ, Cammi R, Pomelli C, Ochterski JW, Ayala PY, Morokuma K, Voth GA, Salvador P, Dannenberg JJ, Zakrzewski VG, Dapprich S, Daniels AD, Strain MC, Farkas O, Malick DK, Rabuck AD, Raghavachari K, Foresman JB, Ortiz JV, Cui Q, Baboul AG, Clifford S, Cioslowski J, Stefanov BB, Liu G, Liashenko A, Piskorz P, Komaromi I, Martin RL, Fox DJ, Keith T, Al-Laham MA, Peng CY, Nanayakkara A, Challacombe M, Gill PMW, Johnson B, Chen W, Wong MW, Gonzalez C, Pople JA (2004) Gaussian 03, revision E.01. Gaussian, Inc., Wallingford, CT
71. Lee C, Yang W, Parr RG (1988) Phys Rev B 37:785–789
72. Becke AD (1993) J Chem Phys 98:5648–5652
73. Perdew JP, Burke K, Ernzerhof M (1996) Phys Rev Lett 77:3865–3868
74. Perdew JP, Burke K, Ernzerhof M (1997) Phys Rev Lett 78:1396
75. Adamo C, Barone V (1999) J Chem Phys 110:6158–6169
76. Weigend F, Ahlrichs R (2005) Phys Chem Chem Phys 7:3297–3305
77. Ahlrichs R, Bär M, Häser M, Horn H, Kölmel C (1989) Chem Phys Lett 162:165–169
78. Eichkorn K, Weigend F, Treutler O, Ahlrichs R (1997) Theor Chem Acc 97:119–124

79. Weigend F, Häser M, Patzelt H, Ahlrichs R (1998) Chem Phys Lett 294:143–152
80. Schaefer A, Huber C, Ahlrichs R (1992) J Chem Phys 97: 2571–2577
81. Schaefer A, Huber C, Ahlrichs R (1994) J Chem Phys 100: 5829–5835
82. Weigend F, Furche F, Ahlrichs R (2003) J Chem Phys 119: 12753–12762
83. van Koningsveld H (1990) Acta Cryst B46:731–735
84. Boys SF, Bernardi F (1970) Mol Phys 19:553–566
85. Macrae CF, Bruno IJ, Chisholm JA, Edgington PR, McCabe P, Pidcock E, Rodriguez-Monge L, Taylor R, van de Streek J, Wood PA (2008) J Appl Cryst 41:466–470
86. Nachtigall P, Bulánek R (2006) Appl Catal A General 307:118–127
87. Rejmak P, Sierka M, Sauer J (2007) Phys Chem Chem Phys 9:5446–5456
88. Rejmak P, Broklawik E, Góra-Marek K, Radoń M, Datka J (2008) J Phys Chem C 112:17998–18010
89. Gervasini A, Picciau C, Auroux A (2000) Microporous Mesoporous Mater 35–36:457–469
90. Irikura KK (2007) J Phys Chem Ref Data 36(2):389–397
91. Aylor AW, Larsen SC, Reimer JA, Bell AT (1995) J Catal 157:592–602